

X-ray Spectroscopy of the O2If* Star HD 93129A

David H. Cohen¹

¹*Swarthmore College, Department of Physics and Astronomy, 500 College Ave., Swarthmore PA 19081, USA*

Abstract. The O2If* star, HD 93129A, is among the earliest in the Galaxy and has one of the strongest winds of any O star. In this paper, we show that its hard and strong X-ray emission can be understood in terms of the standard embedded wind shock paradigm for effectively single, hot, massive stars. Wind attenuation of the intrinsically soft X-ray emission is an important effect, which explains the hardness of the observed X-rays. We measure the degree of wind absorption in two different ways in order to derive a mass-loss rate of roughly $6 \times 10^{-6} M_{\odot} \text{ yr}^{-1}$. This value is consistent with the observed H α line if a clumping factor of $f_{\text{cl}} = 12$ is assumed.

1. Introduction

HD 93129A is one of the earliest type stars in the Galaxy, and has perhaps the most powerful stellar wind measured in an O star, with a terminal velocity of $v_{\infty} = 3200 \text{ km s}^{-1}$ and a mass-loss rate¹ of $\dot{M} \approx 2 \times 10^{-5} M_{\odot} \text{ yr}^{-1}$ (Taresch et al. 1997; Repolust et al. 2004). The star is a strong source of hard X-rays, which have traditionally been attributed to colliding wind shocks in a close binary².

The X-ray luminosity, while high ($L_X = 7 \times 10^{32} \text{ ergs s}^{-1}$), is roughly consistent with the standard $L_X/L_{\text{bol}} = 10^{-7}$ relationship seen for most O stars, where the X-rays arise in Embedded Wind Shocks (EWS), related to the Line-Driving Instability (LDI). In this paper, we investigate the extent to which the X-ray properties of HD 93129A can be explained by the standard EWS paradigm. We do this by accounting for wind attenuation of the X-rays in both a broad-band X-ray spectral analysis, using the newly developed *windtabs* model for wind attenuation (Leutenegger et al. 2010), and also by an analysis of individual X-ray line profile shapes. Detailed results were presented recently in Cohen et al. (2011), so here we present an overview.

¹The mass-loss rates traditionally found in the literature are derived from the H α emission, but assume a smooth wind, neglecting clumping effects on this density-squared diagnostic.

²The visual companion, HD 93129B, at a separation of $2.7''$, is too distant from the primary (5500 AU) to have significant wind-wind interactions with HD 93129A. However, a closer companion, detected with the HST FGS (Nelan et al. 2004), with a separation of only $0.05''$, corresponding to 100 AU, could be a source of the colliding-wind X-rays (Evans et al. 2003).

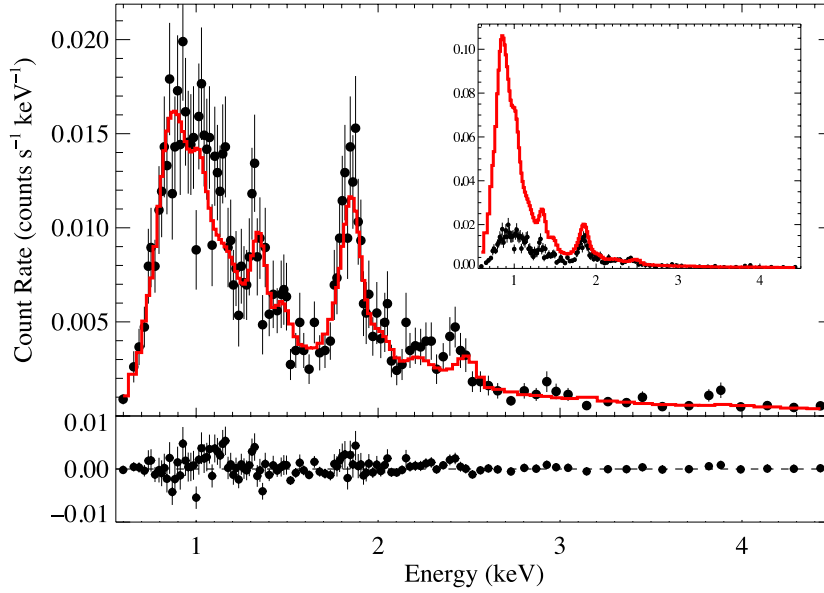


Figure 1. The zeroth order ACIS CCD spectrum, along with the best-fit two-temperature *apec* thermal emission model, including absorption by both the stellar wind and the ISM (histogram). The vast majority of the emission in this spectrum is line emission, but due to the low resolution of the detector as well as the presence of many weak, blended lines, the spectrum looks relatively smooth. The inset figure shows the same data with a model identical to the best-fit model, except that the wind absorption (Σ_w in *windtabs*) is zeroed out. This model spectrum makes the significance of the wind absorption effect quite obvious. Nearly 80% of the emitted EWS X-rays are absorbed before they can escape from the wind.

2. Broadband X-ray Spectral Distribution

X-ray absorption is traditionally modeled using one of several tools developed for interstellar attenuation of X-rays. Such models have recently been shown to be inadequate for modeling wind attenuation (Leutenegger et al. 2010) for two reasons: (1) the transmission of the wind falls with optical depth much more slowly than the standard $\exp(-\tau)$ relation when the emitting plasma is intermixed with the absorbing plasma, unlike the ISM, where the emitter is entirely behind the absorbing medium, and (2) the wind's opacity is lower than that of the ISM because the wind is partially ionized (and specifically, H and He are fully ionized, eliminating them as sources of bound-free opacity). Here we employ the *windtabs* absorption model (Leutenegger et al. 2010), which accounts both for the radiation transport of a distributed emitter and the opacity of stellar wind material, in conjunction with an *apec* thermal emission model (Smith et al. 2001), to fit the low-resolution *Chandra* ACIS CCD spectrum of HD 93129A.

We fit a model that has two separate *apec* emission components, one attenuated both by the wind and the ISM (to model the EWS X-ray contribution) and one attenuated only by the ISM (to model the Colliding Wind Shock (CWS) emission). Each emission component has two free parameters: a temperature and a normalization. The *windtabs* model has only one free parameter: the wind mass-column density,

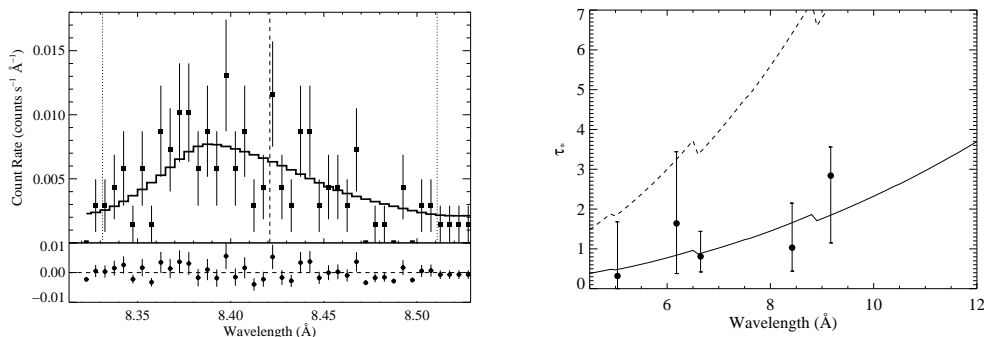


Figure 2. The *Chandra* Medium Energy Grating data for the Lyman- α line of Mg XII, along with the best-fit model (left). The laboratory rest wavelength of each line is indicated by a vertical dashed line and the Doppler shifts associated with the (positive and negative) terminal velocity are indicated by the vertical dotted lines. The five τ_* values fit with a single opacity model in order to derive \dot{M} are shown on the right. The best-fit τ_* model ($\dot{M} = 6.8 \times 10^{-6} M_{\odot} \text{ yr}^{-1}$) is shown as a solid line, while the dotted line represents the form of τ_* that would be expected if the traditional mass-loss rate of $2.6 \times 10^{-5} M_{\odot} \text{ yr}^{-1}$ (Repolust et al. 2004) were correct.

$\Sigma_* \equiv \dot{M}/4\pi R_* v_{\infty}$. The best-fit model along with the ACIS data is shown in Fig. 1. The EWS component has a temperature of 0.6 keV and a wind mass column of $\Sigma_* = 0.052 \text{ g cm}^{-2}$, while the CWS component has a temperature of 3.3 keV but only 5% the normalization of the cooler component. This indicates that the vast majority of the X-ray emission can be attributed to the standard EWS mechanism, with only a very small contribution from the CWS mechanism. The temperature of the dominant component, 0.6 keV, is consistent with the relatively low emission temperatures expected from the EWS mechanism. Indeed, the hardness of the observed X-rays is due to wind absorption and not to intrinsically high temperatures. The amount of wind attenuation we find is quite significant, as can be seen in the inset to Fig. 1, where we show the same model but with the wind attenuation zeroed out. Note that nearly 80% of the X-ray emission is absorbed by the wind. Because wind X-ray opacity is higher at lower energies, the significant wind attenuation hardens the emergent X-rays significantly.

The wind mass column density we find from the fit corresponds to a mass-loss rate of $\dot{M} = 5.2 \times 10^{-6} M_{\odot} \text{ yr}^{-1}$; about four times lower than the traditional unclumped H α mass-loss rate. We independently check this result in the next section, where we present fits to the individual X-ray emission line profiles.

3. X-ray Line Profiles

The shapes of O star X-ray emission lines are characteristically blue-shifted, and skewed, due to the preferential attenuation of red-shifted photons emitted by the far hemisphere of the wind, compared to the blue-shifted photons emitted by the near hemisphere. The degree of shift and asymmetry is proportional to the parameter $\tau_* \equiv \kappa \Sigma_* = \kappa \dot{M}/4\pi R_* v_{\infty}$, and thus if the stellar radius, R_* , the wind terminal velocity, v_{∞} , and the wind opacity, κ , are known, this parameter gives the mass-loss rate directly. Note that the wind opacity

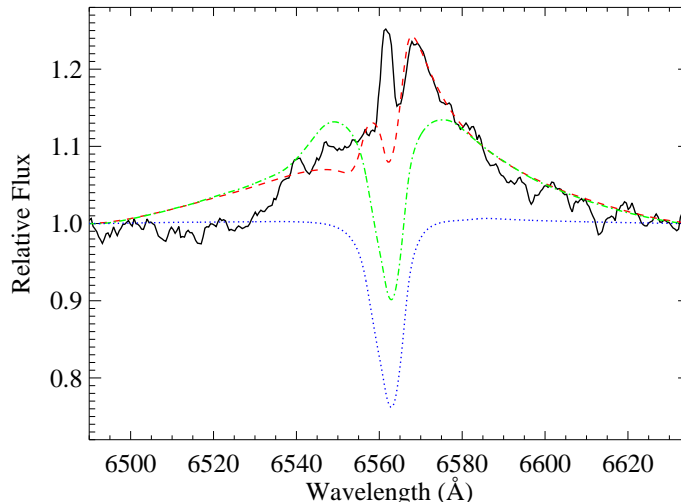


Figure 3. The $H\alpha$ emission profile (black, solid) is well reproduced by a model that includes clumping beginning at a radius of $R_{cl} = 1.05 R_*$ (red, dashed). The model with $R_{cl} = 1.3 R_*$ (green, dash-dot) does not have enough emission in the line core. For comparison, we show a model with no clumping (blue, dotted), in which the model fails to produce any emission. All models have $\dot{M} = 7 \times 10^{-6} M_{\odot} \text{ yr}^{-1}$ and $\beta = 0.7$. And the two models with clumping have $f_{cl} = 12$. Note that the narrow emission peak at line center likely has a significant contribution from nebular emission, which we do not model.

varies with wavelength, so each line should have a different τ_* value. A multiplexing advantage can be realized if all the τ_* values are fit simultaneously for a single mass-loss rate. We show our fit to the profile of the strongest line, Mg XII , measured with the *Chandra* MEG grating, in Fig. 2. There we also show the τ_* values derived from all the emission lines in the grating spectrum of HD 93129A as a function of wavelength, with the best-fit mass-loss rate model superimposed.

The best-fit model has $\dot{M} = 6.8 \times 10^{-6} M_{\odot} \text{ yr}^{-1}$, in good agreement with the value from the broadband fitting described in the previous section. The line-profile fitting also provides an estimate of the onset radius of X-ray emission, essentially via the line widths, which will be broader if the onset radius is higher, where the wind velocity is also higher, and lower for a lower onset radius where the wind is slower. We find an average onset radius of $R_o = 1.4 R_*$ for the lines we fit, which is consistent with the results from numerical simulations of the LDI (Feldmeier et al. 1997; Runacres & Owocki 2002).

4. Conclusions

Despite the fact that the O2 If* star, HD 93129A, has quite hard X-ray emission, the observed X-ray properties are well explained in the context of the standard picture of embedded wind shocks in massive stars. The strong, dense wind significantly attenu-

ates the intrinsically soft X-ray emission and in doing so, hardens the X-ray spectrum. The degree of X-ray absorption provides information about the mass-loss rate in two independent ways. Both of these measurements agree, with a mass-loss rate between 5 and $7 \times 10^{-6} M_{\odot} \text{ yr}^{-1}$, representing a reduction of about a factor of four compared to the standard, unclumped $H\alpha$ mass-loss rate, a result that is similar to that found for ζ Pup (Cohen et al. 2010).

The $H\alpha$ emission is well reproduced by this lower mass-loss rate if a clumping factor of $f_{\text{cl}} \equiv \langle \rho^2 \rangle / \langle \rho \rangle^2 = 12$ is assumed. This level of wind clumping must start at just $r = R_{\text{cl}} = 1.05 R_*$ in order to reproduce the core of the $H\alpha$ line. A theoretical $H\alpha$ profile with these model parameters is shown in Fig. 3, compared to the observed profile, and with several other models also shown for comparison. We note that this clumping onset radius is significantly lower than the X-ray onset radius, indicating that wind clumps form close to the photosphere, but are not associated with shocks strong enough to produce X-rays in that location.

In closing, HD 93129A, despite its extreme stellar and wind properties, has X-ray emission that can be well understood in terms of the standard embedded wind shock paradigm. And its mass-loss rate, like those of other O supergiants, must be revised downward by a factor of several due to wind clumping.

Acknowledgments. We acknowledge support from NASA grant NNX11AD26G to Swarthmore College.

References

- Cohen, D. H., Gagné, M., Leutenegger, M. A., MacArthur, J. P., Wollman, E. E., Sundqvist, J. O., Fullerton, A. W., & Owocki, S. P. 2011, *MNRAS*, 415, 3354. [1104.4786](#)
- Cohen, D. H., Leutenegger, M. A., Wollman, E. E., Zsargó, J., Hillier, D. J., Townsend, R. H. D., & Owocki, S. P. 2010, *MNRAS*, 405, 2391. [1003.0892](#)
- Evans, N. R., Seward, F. D., Krauss, M. I., Isobe, T., Nichols, J., Schlegel, E. M., & Wolk, S. J. 2003, *ApJ*, 589, 509. [arXiv:astro-ph/0301485](#)
- Feldmeier, A., Puls, J., & Pauldrach, A. W. A. 1997, *A&A*, 322, 878
- Leutenegger, M. A., Cohen, D. H., Zsargó, J., Martell, E. M., MacArthur, J. P., Owocki, S. P., Gagné, M., & Hillier, D. J. 2010, *ApJ*, 719, 1767. [1007.0783](#)
- Nelan, E. P., Walborn, N. R., Wallace, D. J., Moffat, A. F. J., Makidon, R. B., Gies, D. R., & Panagia, N. 2004, *AJ*, 128, 323
- Repolust, T., Puls, J., & Herrero, A. 2004, *A&A*, 415, 349
- Runacres, M. C., & Owocki, S. P. 2002, *A&A*, 381, 1015
- Smith, R. K., Brickhouse, N. S., Liedahl, D. A., & Raymond, J. C. 2001, *ApJ*, 556, L91. [arXiv:astro-ph/0106478](#)
- Taresch, G., Kudritzki, R. P., Hurwitz, M., Bowyer, S., Pauldrach, A. W. A., Puls, J., Butler, K., Lennon, D. J., & Haser, S. M. 1997, *A&A*, 321, 531